ISSN 2229-5518

Wavelength Dependence of Cloud Depolarization Ratio Due to Multiple Scattering Using A Two-Field-of-View White Light Lidar System

Toshihiro Somekawa, Chihiro Yamanaka, Masayuki Fujita, Edgar A. Vallar, and Maria Cecilia Galvez

Abstract— We presented and analyzed the depolarization ratio at three-wavelengths (450, 550, and 800 nm) using a two-field-of view (FOV) white light lidar system. A simple two-FOV model was used to investigate the effect of multiple scattering on the depolarization ratio. This approach allows us to evaluate the wavelength dependence of the contribution of multiple scattering to the depolarization ratio of clouds.

Index Terms— lidar, depolarization ratio, multiple scattering, field-of-view, angstrom coefficient, white light, femtosecond laser

1 INTRODUCTION

The information content of lidar signals is enhanced by adding depolarization measurements. This principle of operation is well known and based on the simple fact that single backscattered light from spherical particles retains the polarization of the incident light, but irregularly shaped particles cause significant depolarization. Backscattered light from spherical particles also become depolarized if the receiver field-of-view (FOV) is large since the backscattered light includes multiple scattering not only at 180o but also at other scattering angles [1],[2]. However, this opens up the possibility to retrieve the additional information about cloud droplet size or the particle size density distribution by determining the characteristics depolarization ratio due to multiple scattering [3],[4].

In this paper, we report for the first time the wavelength dependence of the effect of multiply scattered lidar returns on the depolarization ratio. The lidar observations are performed using a two-FOV three-wavelength depolarization white light lidar system [5]. The white light lidar system facilitates multi-wavelength measurements of the atmospheric lidar signals because of a broadband light source from 300 nm to more than 950 nm. We evaluate the optical depth from difference in two-FOV depolarization ratio.

Toshihiro Somekawa received his PhD in science from Osaka University, Japan, in 2008. His research now focuses on development of multi-wavelength lidar using a white light continuum and submarine Raman lidar.
E-mail: somekawat@ile.osaka-u.ac.jp

Chihiro Yamanaka received his Ph.D in 1990 for the study of metal vapor lasers from Osaka University, Japan, His research covers electron spin resonance, radiation dosimetry in earth/environmental science, femto laser applications including lidar and laser induced breakdown spectroscopy.

Masayuki Fujita received his PhD in electrical engineering from University of Alberta, Canada, in 1992. He is involved in high-power laser development and short pulse laser applications.

Edgar A. Vallar is an Associate Professor of the Physics Department, De La Salle University, Manila, Philippines. His current research focuses on air quality and health. He employs LIDAR, Sunphotometry, Air Sampling and Modeling in studying the air quality of Manila.

Maria Cecilia D. Galvez is an Associate Professor of the Physics Department, De La Salle University, Manila, Philippines. Her research is on the applications of laser in environment, water and air quality monitoring and measurement using remote sensing and air sampling techniques.
Email:maria.cecilia.galvez@dlsu.edu.ph

2 METHODOLOGY

2.1 Experiment

We performed the lidar experiment using a Ti:sapphire chirped-pulse amplification (CPA) laser system. The femtosecond laser source is a combination of a Ti:sapphire oscillator pumped by a laser diode(LD)-pumped green Nd:YVO4 cw-laser and a regenerative amplifier pumped by a LD-pumped green Nd:YLF laser operated at 1 kHz. This beam is sent to a four-pass Ti:sapphire amplifier which is pumped by the se second harmonic of two Nd:YAG lasers. The final output energy is about 100 mJ per pulse with a pulsewidth of 100 fs and a repetition rate of 10 Hz. This femtosecond terawatt laser

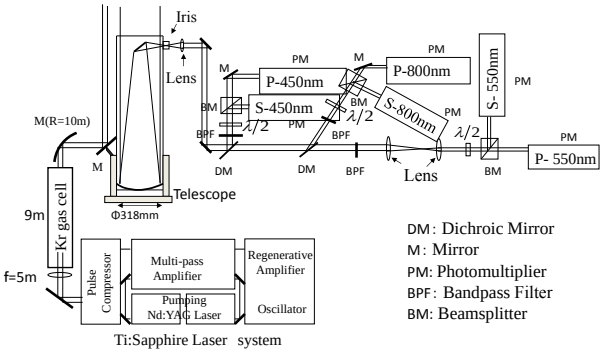

Fig. 1. Schematic diagram of the two-FOV white light lidar system showing both the transmitter and the three wavelength depolarization backscattering spectrometer.

pulse is focused by a lens with a focal length of 5 m into 9-m-long Kr gas cell and converted into the white light continuum which has a linear polarization similar to the original 800 nm. The output beam was transmitted to the atmosphere collinearly to the axis of the receiver telescope with a 30 cm diameter. Backscattered light passes along a light guide consisting of a pair of mirror star diagonals and is then directed to a 3-wavelength depolarization backscattering spectrometer. Figure 1 shows the two-FOV white light lidar system including the transmitter and the 3-wavelength depolarization backscattering spectrometer. The light is spectrally separated by means of dichroic mirrors and band-pass filters. A λ/2 plate is placed to line up the polarization axis of the spectrometer with the polarization vector of the transmitted light. A polarizing beamsplitter cube separates P- and S-polarized light at each wavelength. The detectors are 28-mm diameters photomultiplier tubes used in the analog mode. This detection unit is aligned by a He-Ne laser. Wavelength properties of the filters, the half-wave plates and beamsplitter cubes are given in Table 1. In order to detect the more intense signals, the band-pass filter and the half-wave plate at 550 nm have a broadband effective wavelength. The FOV was varied using an iris diaphragm placed at the focal plane of the receiving telescope. Lidar measurements for FOVs 1.6 and 4.0 mrad were conducted consecutively with an interval of 1 minute between the two FOVs.

TABLE 1
SPECTRAL SPECIFICATION OF SOME OPTICAL COMPONENTS IN EACH CHANNEL

Wavelength Channel		450	550	800
Band-pass Filter	Center Wavelength	457.9 nm	550 nm	800 nm
	FWHM (nm)	10	50	10
Half-wave Plate		449 - 467	460 – 655	784 – 816
Beamsplitter cube		420 – 680	420 – 680	620 – 1000

2.2 Two Field-of-View Model

To study the wavelength dependence of cloud depolarization due to multiple scattering, we need to obtain from the lidar observation, the depolarization ratio due mainly on multiple scattering. To do this we introduce a simple two-FOV model where we use the observed the depolarization ratio at two FOVs, small (SF) and large (LF). The method is described in this section. The total range squared corrected lidar scaterring signal is equal to

$$I_i = I_{i,P} + I_{i,S} = I_{i,P}\left(1+\delta_i\right) \tag{1}$$

where the subscript i is equal to SF or LF for smaller or larger FOV, respectively, and $I_{i,P}$ and $I_{i,S}$ are the parallel and perpendicular components of the backscattered intensity, respectively for each of the FOV. The lidar depolarization ratio, δ_i, is given by

$$\delta_i = \frac{I_{i,S}}{I_{i,P}} \tag{2}$$

We can introduce the multiple-scattering fraction, Y, such that

$$Y = \frac{I_{SF}}{I_{LF}} \tag{3}$$

where I_{SF} and I_{LF} are the total range squared corrected scatter scattering signal (single + multiple) lidar backscatter signal at smaller and larger FOV, respectively. And we can also have sets equation representing the difference between I_{SF} and I_{LF} range squared corrected lidar scattering signal given by the following:

$$\begin{aligned} I_M &= I_{LF} - I_{SF} \\ I_{M,P} &= I_{LF,P} - I_{SF,P} \\ I_{M,S} &= I_{LF,S} - I_{SF,S} \\ \delta_M &= \frac{I_{M,S}}{I_{M,P}} \end{aligned} \tag{4}$$

where I_M represents the difference. From (1) and (4) one can obtain $I_{LF,P}$.

$$\begin{aligned} I_{LF,P} &= I_{SF,P} + I_{M,P} \\ I_{LF,P} &= I_{SF}\left(\frac{1}{1+\delta_{SF}}\right) + I_M\left(\frac{1}{1+\delta_M}\right) \end{aligned} \tag{5}$$

Using (3) into (5)

$$I_{LF,P} = \left(\frac{I_{LF}Y}{1+\delta_{SF}}\right) + \left(\frac{I_{LF}\left(1-Y\right)}{1+\delta_M}\right) \tag{6}$$

Similarly for $I_{LF,S}$

$$I_{LF,S} = \left(\frac{\delta_{SF} I_{LF} Y}{1+\delta_{SF}}\right) + \left(\frac{\delta_M I_{LF}\left(1-Y\right)}{1+\delta_M}\right) \tag{7}$$

Dividing (7) and (6), we can obtain

$$\delta_{LF} = \frac{\delta_M\left(1+\delta_{SF}\right) + Y\left(\delta_{SF} - \delta_M\right)}{\left(1+\delta_{SF}\right) - Y\left(\delta_{SF} - \delta_M\right)} \tag{8}$$

From (8), we can obtain, the depolarization ratio due mainly to multiple scattering and this is given by:

$$\delta_M = \frac{\delta_{LF}\left(1+\delta_{SF} - Y\delta_{SF}\right) - Y\delta_{SF}}{\left(1+\delta_{SF}\right) - Y\left(1+\delta_{LF}\right)} \tag{9}$$

where δ_{SF} and δ_{LF} are the observed depolarization ratio for smaller and larger field of view, respectively, which can be obtained from lidar measurement. To make sure that lidar return signal from the two FOVs are coming from the same size distribution, we make use of the angstrom coefficient, $\mathring{a}$, which is a good indicator of particle size and is defined below:

$$\overset{o}{a}_{550/800} = -\frac{\ln[\beta(550)/\beta(800)]}{\ln(550/800)} \quad (10)$$

where β(λ) is the backscatter coefficient for λ equal to 550 nm and 800 nm, and it is calculated from (1) using the algorithm of Fernald [7].

3 Results and Discussion

Figure 2 shows the time height display of the depolarization ratios at 450, 550, and 800 nm observed in Osaka, Japan, in February 2007 for two FOVs, 1.6 and 4.0 mrad, which represents the SF and LF, respectively. 800P presents the time height display of the range squared corrected signal, which serves as a reference profile for the atmospheric information during the observation period. It can be seen from Fig. 2 that on 2 February 2007, thin clouds with thickness of about 300 m were identified at about 1.0 km altitude during the two FOV measurement. An aerosol layer was identified below the clouds. Figure 3(a) shows the maximum depolarization ratio obtained from cloud signals for each measurement as a function of wavelength. Since multiple scattering in multi cloud layer are expected to have a more complex effect, we discussed only the measurement obtained for a single cloud layer. It can be seen that from Fig. 3(a), that depolarization ratios

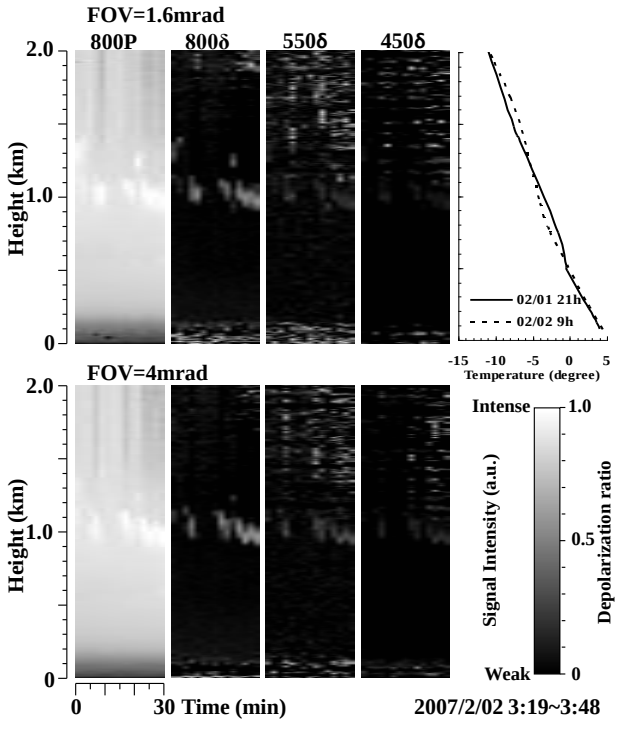

Fig. 2. Time height displays from the white light lidar measurement on February 2, 2007 using two different FOVs, 1.6 mrad and 4.0 mrad. Shown at top and bottom are grey-scale displays of the range squared corrected signals at 800 nm in logarithmic units and the depolarization ratios at 450, 550, and 800 nm. The temperature profile at Shionomisaki station taken on the same day and close to the time of our lidar measurements is also presented on the upper right.

with 4.0-mrad FOV were larger than that with 1.6-mrad FOV. These results seem to be in good agreement with the previous paper where the depolarization signals were induced by multiple scattering [6]. Also, in Fig. 3(b), the corresponding Angstrom coefficients for this observation are presented. In our previous paper [5], we showed a positive correlation between Angstrom coefficient and depolarization ratio. The Angstrom coefficient for the 4.0-mrad FOV, as seen from Fig. 3, is larger compared to 1.6-mrad FOV. Since the Angstrom coefficients showed the same tendency as the depolarization ratios, the difference in the depolarization ratio between the two FOVs presented in fig. 3 is attributed mainly to the temporal variations in cloud particle size. Thus, in order to determine the change in the depolarization ratio due mainly to multiple scattering, it is necessary to compare lidar return signals from the two FOV measurements with the same size distribution.

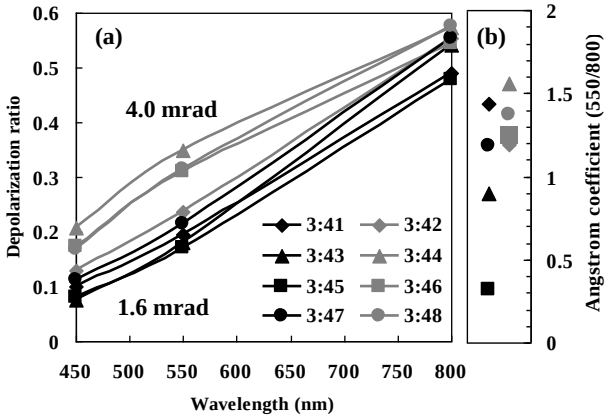

Fig. 3. (a) Measured depolarization ratios as functions of wavelength and (b) corresponding Angstrom coefficients. Black and gray symbols denote 1.6 and 4.0 mrad FOV measurements, respectively.

Figure 4 shows the maximum depolarization ratio obtained from cloud signals for 1.6- and 4.0-mrad measurements with almost the same angstrom coefficients. The Angstrom coefficients were 0.877, 0.901, 1.19 and 1.19 for lidar signals observed at 3:36, 3:43, 3:42 and 3:47, respectively, with a standard deviation of 0.044. Hence, we can assume that they have same size distribution. Since the depolarization ratio with a large FOV, $\delta_{4.0}$, involves that with a small FOV, $\delta_{1.6}$, we can obtain the depolarization ratios due to multiple scattering, δ_M, from (9). Figure 4(c) shows the wavelength dependence of the normalized multiple scattering depolarization ratios. The parameter $\delta_M/\delta_{1.6}$ is utilized in conjunction with $\delta_{1.6}$ to characterize more fully the wavelength dependence of δ_M. The values of $\delta_M/\delta_{1.6}$ were observed to be increasing with decreasing wavelength. The differences in $\delta_M/\delta_{1.6}$ at small wavelength are likely to be due to the wavelength dependence in the multiple scattering as a result of the wavelength dependence on forward scattering [8].

The multiple scattering seems to be associated with the change in optical depth that results from a change in particle number density. The relationship of the particle size and optical depth is reported to be a negative correlation such that the particle size increases as the optical depth decreases [9].

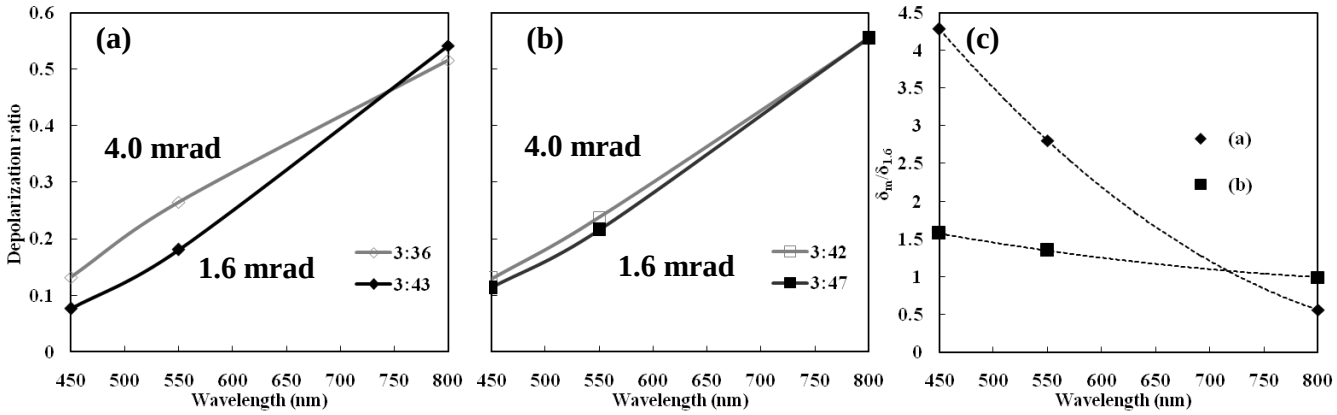

Fig. 4. (a), (b) The wavelength dependence of the measured depolarization ratios for receiver FOVs of 1.6 and 4.0 mrad having almost the same size distribution. (c) The wavelength dependence of ratios of multiple-scattering (δM) to the narrow FOV (δ1.6) depolarization ratio at cloud.

Therefore, as already seen from the Angstrom coefficients, the optical depth in Fig. 4(a) may be smaller than that in Fig. 4(b) considering that the Angstrom coefficients are larger in a smaller particle size. The calculated optical depth, which is the integral of the extinction coefficient from cloud bottom to cloud top, at 1.6-mrad FOV in Fig. 4(a) and Fig. 4(b) was determined to be 0.73 and 0.78 at 800 nm, respectively. Thus, in the low optical depth cloud as shown by ◆ symbols in Fig. 4(c), the $\delta_M/\delta_{1.6}$ values show a large increasing trend as the effect of the above-mentioned forward scattering becomes more dominant. On the other hand, the depolarization ratio δ_M approaches the value for backscattering at 180° for greater penetration depth [10]. In the cloud of large optical depth the penetration depth may be considered to be greater than in clouds with small optical depth. As a result, the values of $\delta_M/\delta_{1.6}$ have a small slope and approaching a value of 1. Even though the assumptions made here are oversimplified and the comparison between the FOV is only based on two particular clouds observed during lidar measurements on 2 February 2007, the variations in $\delta_M/\delta_{1.6}$ contain retrievable information on cloud parameter such as optical depth and droplet size. Long-term measurements of clouds and aerosols with the use of a depolarization lidar with an adjustable FOV would provide a robust means of measuring some relevant parameters.

4 Conclusion

As a preliminary test of the multiple scattering depolarization ratio routines outlined in this paper, the two-FOV data from the white light depolarization lidar experiments were analyzed. This approach allows us to evaluate the multiple scattering contributions to the lidar depolarization ratio. In agreement with our expectations concerning the wavelength dependence of depolarization ratios, the approximate multiple-single scattering ratio $\delta_M/\delta_{1.6}$ was seen to increase quadratically with decreasing wavelength as shown in Fig. 4(c). This seems to suggest that the curvature in $\delta_M/\delta_{1.6}$ may lead to the identification of some atmospheric parameters. Such future enhancements to the white light lidar technique should allow improved simultaneous measurements of the particle size, shape, and the number density.

Acknowledgment

This work has been performed within the framework of joint research with the Institute of Laser Engineering, Osaka University, 2005-2007.

References

[1] K. Sassen and H. Zhao, "Lidar multiple scattering in water droplet clouds: Toward an improved treatment," *Opt. Rev.*, 5 , pp. 394-400, 1995.

[2] L. R. Bissonnette and G. Roy, "Range-height scans of lidar depolarization for characterizing properties and phase of clouds and precipitation," *J. Atmos. Ocean. Technol.*, 18, pp. 1429-1446 , 2001.

[3] E. W. Eloranta, "Practical model for the calculation of multiply scattered lidar returns," *Appl. Opt.*, 37 (1998), pp. 2464-2472.

[4] B. Tatarov, T. Trifonov, B. Kaprielov, and I. Kolev, "Dependence of the lidar signal depolarization on the receiver's field of view in the sounding of fog and clouds," Appl. Phys. B 71 (2000), pp. 593-600.

[5] T. Somekawa, C. Yamanaka, M. Fujita, and M. C. Galvez, "Simultaneous three-wavelength depolarization measurements of clouds and aerosols using a coherent white light continuum," J. Appl. Phys., 103 (2008) 043101.

[6] S. R. Pal and A. I. Carswell, "Polarization properties of lidar scattering from clouds," Appl. Opt., 12 (1973), pp. 1530-1535.

[7] F. G. Fernald, "Analysis of atmosphere lidar observations: some comments," Appl. Opt., 23 (1984), pp. 652-653.

[8] S. R. Pal and A. I. Carswell, "Polarization properties of lidar scattering from clouds at 347 nm and 694 nm," Appl. Opt., 17 (1978), pp. 2321-2328.

[9] T. Nakajima, M. D. King, J. D. Spinhirne, and L. F. Radke, "Detection of the optical thickness and effective particle radius of clouds from reflected solar radiation measurements. Part II: Marine stratocumulus observations," J. Atmos. Sci., 48 (1991), pp. 728-750.

[10] S. Reichardt and J. Reichardt, "Effect of multiple scattering on depolarization measurements with spaceborne lidars," Appl. Opt., 42 (2003), pp. 3620-3633.